

# Activity-dependent nuclear translocation and intranuclear distribution of NFATc in adult skeletal muscle fibers

Yewei Liu,<sup>1</sup> Zoltán Cseresnyés,<sup>1</sup> William R. Randall,<sup>2</sup> and Martin F. Schneider<sup>1</sup>

<sup>1</sup>Departments of Biochemistry and Molecular Biology, and <sup>2</sup>Department of Pharmacology and Experimental Therapeutics, University of Maryland School of Medicine, Baltimore, MD 21201

**T**ranscription factor nuclear factor of activated T cells NFATc (NFATc1, NFAT2) may contribute to slow-twitch skeletal muscle fiber type-specific gene expression. Green fluorescence protein (GFP) or FLAG fusion proteins of either wild-type or constitutively active mutant NFATc [NFATc(S→A)] were expressed in cultured adult mouse skeletal muscle fibers from flexor digitorum brevis (predominantly fast-twitch). Unstimulated fibers expressing NFATc(S→A) exhibited a distinct intranuclear pattern of NFATc foci. In unstimulated fibers expressing NFATc-GFP, fluorescence was localized at the sarcomeric z-lines and absent from nuclei. Electrical stimulation using activity patterns typical of slow-twitch muscle, either continu-

ously at 10 Hz or in 5-s trains at 10 Hz every 50 s, caused cyclosporin A-sensitive appearance of fluorescent foci of NFATc-GFP in all nuclei. Fluorescence of nuclear foci increased during the first hour of stimulation and then remained constant during a second hour of stimulation. Kinase inhibitors and ionomycin caused appearance of nuclear foci of NFATc-GFP without electrical stimulation. Nuclear translocation of NFATc-GFP did not occur with either continuous 1 Hz stimulation or with the fast-twitch fiber activity pattern of 0.1-s trains at 50 Hz every 50 s. The stimulation pattern-dependent nuclear translocation of NFATc demonstrated here could thus contribute to fast-twitch to slow-twitch fiber type transformation.

## Introduction

Skeletal muscle fibers have been classified into fiber types based on contraction speed and metabolic capacity (Pette and Staron, 1990). The three classical fiber types are fast-twitch glycolytic (type IIB), fast-twitch oxidative/glycolytic (type IIA), and slow-twitch oxidative (type I), which vary from high to low, respectively, in fiber diameter, fiber force production, speed of contraction, and rapidity of activation and relaxation, and systematically from low to high in oxidative capacity and fatigue resistance. Fiber type is determined by the expression of fiber type-specific isoforms of almost all muscle proteins, including contractile proteins, regulatory proteins, and metabolic enzymes (Schiaffino and Reggiani, 1996).

Muscle fiber type and fiber type-specific protein expression can be modulated over periods of weeks or months depending on the activity pattern of the fiber (Lomo et al.,

1974; Salmons and Sreter, 1976; Pette and Vrbova, 1992; Pette and Staron, 1997). Physiologically, this activity pattern is set by the firing pattern in the motor neuron innervating the muscle fiber (Hennig and Lomo, 1985). Neurons innervating slow-twitch fibers exhibit action potentials at relatively low, but sustained rates. In contrast, neurons to fast-twitch fibers exhibit action potential patterns consisting of occasional bursts of activity at relatively high frequencies, interspersed by periods of inactivity. Crossing the nerves innervating muscles having predominantly fast- and slow-twitch fibers results in a gradual transformation of the muscles to the opposite fiber type (Muntener et al., 1985, 1987). Similar fiber transformation can be accomplished by direct electrical stimulation of either the motor nerve to the muscle or the muscle itself with the activity pattern characteristic of the other muscle (Windisch et al., 1998). These protein transformations require weeks or months to occur due to the slow turn over of membrane and contractile filament proteins in adult, fully differentiated muscle. In contrast, the underlying changes in gene expression occur within a few days of changing the activity pattern of the muscle (Peuker and Pette, 1995; Barton-Davis et al., 1996).

Address correspondence to Martin F. Schneider, Department of Biochemistry and Molecular Biology, University of Maryland School of Medicine, 108 North Greene St., Baltimore, MD 21201-1503. Tel.: (410) 706-7812. Fax: (410) 706-8297. E-mail: mschneid@umaryland.edu

Key words: cell nucleus; skeletal muscle; NFAT; cultured cells; electrical stimulation

The signaling pathways regulating fiber type-specific gene expression are beginning to be elucidated. Based on studies on myogenic cell lines, it has been suggested that a major component in the transformation of a fast-twitch to a slow-twitch fiber may involve the transcription factor nuclear factor of activated T cells (NFATc)\* (Chin et al., 1998), which has been extensively studied in relation to T cell activation (Northrop et al., 1994; Crabtree, 1999). Elevated cytosolic  $[Ca^{2+}]$  accompanying T cell activation results in the activation of the  $Ca^{2+}$ -sensitive phosphatase calcineurin. Activated calcineurin dephosphorylates NFATc, removing phosphate groups that mask its nuclear localization signal, thereby enabling its nuclear translocation and its action as a transcription factor (Beals et al., 1997). Five different NFAT genes have been identified thus far: NFATc (NFATc1 or NFAT2), NFATp (NFATc2 or NFAT1), NFAT4 (NFATc3 or NFATx), NFAT3 (NFATc4), and NFAT5 (Rao et al., 1997; Crabtree, 1999; Lopez-Rodriguez et al., 1999). Recent studies have indicated that NFATc, an NFAT isoform present in skeletal muscle, may play a role in fast-twitch to slow-twitch fiber transformation (Chin et al., 1998). The  $Ca^{2+}$ -dependent activation of calcineurin (Dunn et al., 1999; Bigard et al., 2000; Naya et al., 2000) and calcineurin-dependent dephosphorylation and subsequent nuclear translocation of NFAT (Delling et al., 2000; Dunn et al., 2000) has been suggested to be an important step in the signaling pathway for fast- to slow-twitch fiber type transformation. However, other reports have indicated that NFATc may not be a dominant factor (Calvo et al., 1999; Swoap et al., 2000).

We have recently developed an *in vitro* system for maintaining and studying adult rodent fast-twitch skeletal muscle fibers in culture with or without electrical stimulation (Liu et al., 1997; Liu and Schneider, 1998). We now use this system to investigate the nuclear translocation of NFATc in response to various patterns of fiber stimulation and activation. After expressing an NFATc-GFP fusion protein in single adult mouse skeletal muscle fibers in culture, we find that continuous stimulation at 10 Hz to mimic slow-twitch fiber activity (Hennig and Lomo, 1985) caused nuclear translocation of NFATc. We also find that 5-s trains of 10 Hz fiber activity produced by electrical stimulation repeated every 50 s also caused cyclosporin A (CsA)-sensitive nuclear translocation of NFATc. However, the same overall rate of stimulation and muscle activation, but at a constant 1 Hz rate, did not result in any nuclear translocation of NFATc. Application of 0.1 s trains of stimuli at 50 Hz every 50 s to mimic fast-twitch fiber activity (Hennig and Lomo, 1985) also did not result in nuclear translocation. We further find that after nuclear translocation NFATc is localized into discrete intranuclear foci, which may play a role in the regulation of the transcriptional activity of NFATc within the muscle fiber nucleus. Thus, NFATc exhibits a stimulus pattern-dependent nuclear translocation and concentration in distinct intranuclear foci. This activity pattern-dependent

translocation of NFATc may contribute to the control of expression of slow fiber type-specific genes.

## Results

### Fiber distribution of expressed NFATc

As reported previously by our group, the dissociated flexor digitorum brevis (FDB) muscle fibers survived well in culture, with most fibers retaining cross striations and the ability to contract in response to electrical stimulation (Liu et al., 1997). The FDB cultures were infected with recombi-

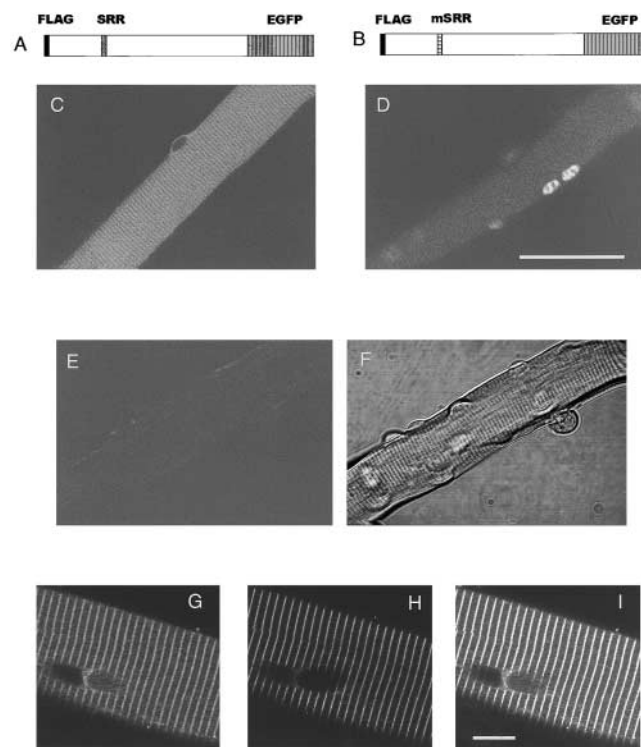


**Figure 1. Cultured adult mouse FDB fibers after viral infection for expression of NFATc-GFP fusion proteins.** (A and B)

Schematic diagram of the expressed FLAG-NFATc-GFP and FLAG-NFATc(S $\rightarrow$ A)-GFP fusion proteins. The positions of the SRR and mutant SRR (mSRR) are indicated. Both of the expressed proteins contain a FLAG epitope tag at the NH<sub>2</sub> terminus and an EGFP at the COOH terminus. FLAG-NFATc(S $\rightarrow$ A) (unpublished data), which lacks the EGFP, was also expressed in some fibers. (C) A living fiber expressing NFATc-GFP exhibited a striped pattern of fluorescence in nonnuclear, sarcomeric regions, but did not have fluorescence in nuclei. (D) A fiber expressing NFATc(S $\rightarrow$ A)-GFP had negligible nonnuclear fluorescence, but had bright nuclei. (E) A living, noninfected fiber had negligible fluorescence. (F) Transmitted light image of the same fiber as in (E). Note that to facilitate the viewing of sarcomeric or nuclear distribution of GFP fluorescence, the pixel value of the fluorescent signal was increased by 55% in all pixels in images (C-E), with any pixels exceeding saturation in the 8-bit image set to the saturation value (white). This possibly nonlinear image manipulation was only applied to panels C-E and was not applied to any other figures in this paper, and not used in any image analyses in this paper. (G-I) A fiber expressing NFATc-GFP (G) was stained with antibody against  $\alpha$ -actinin (H). The overlay (I) indicates that  $\alpha$ -actinin at z-line precisely colocalizes with NFATc-GFP. Bars: (C-E) 50  $\mu$ m; (G-I) 10  $\mu$ m.

\*Abbreviations used in this paper: AOI, area of interest; CsA, cyclosporin A; FDB, flexor digitorum brevis; gal, galactosidase; GFP, green fluorescence protein; MEF2, myocyte enhancer factor 2; NFAT, nuclear factor of activated T cells; SRR, serine-rich region; TTX, tetrodotoxin.

nant adenoviruses as described in Materials and methods. The cultures were kept for another 3 d (~72–76 h) before the experiments were begun and images were taken. Fig. 1 C shows a confocal fluorescence image of an FDB fiber infected with adenovirus-containing NFATc–GFP cDNA (Fig. 1 A). The fiber exhibited a striped pattern of fluorescence throughout the entire fiber cytoplasm, but no fluorescence in the nuclei, which appear dark. This appearance was characteristic of the vast majority of fluorescent fibers in NFATc–GFP-infected unstimulated cultures. The cytosolic fluorescence exhibited a periodic, repeating sarcomeric pattern of sharp fluorescent lines. Based on the colocalization of  $\alpha$ -actinin antibody staining and GFP fluorescence in fibers expressing NFATc–GFP (Fig. 1, G–I), the lines of NFATc–GFP fluorescence are located at the Z-lines at the center of the I band of the sarcomere. Perinuclear fluorescence was also observed in NFATc–GFP-infected fibers (Fig. 1 C). Fig. 1 D presents an FDB fiber 3 d after infection with adenovirus-containing NFATc(S→A)–GFP (Fig. 1 B), a mutant constitutively targeted to the nucleus (Beals et al., 1997). In fibers infected with this construct, fluorescence was concentrated inside nuclei in a nonuniform pattern of distribution, with negligible nonnuclear cytoplasmic fluorescence. This pattern was observed in all fluorescent fibers infected with NFATc(S→A)–GFP. Fig. 1 E is a confocal fluorescence image of a control fiber without virus infection and Fig. 1 F is the image obtained by monitoring the transmitted light intensity of the excitation beam during the confocal scanning of the same fiber.

### Intranuclear distribution of NFATc and nuclear-targeted $\beta$ -galactosidase

We next investigated the intranuclear distribution of NFATc(S→A)–GFP. Fig. 2, A–C present enlarged images of individual nuclei from fibers which were infected with adenovirus-containing NFATc(S→A)–GFP, FLAG–NFATc(S→A), and nuclear-targeted  $\beta$ -galactosidase (gal) cDNA, respectively. Each row presents six nuclei from three different individual fibers. As illustrated in Fig. 2 A, the intranu-

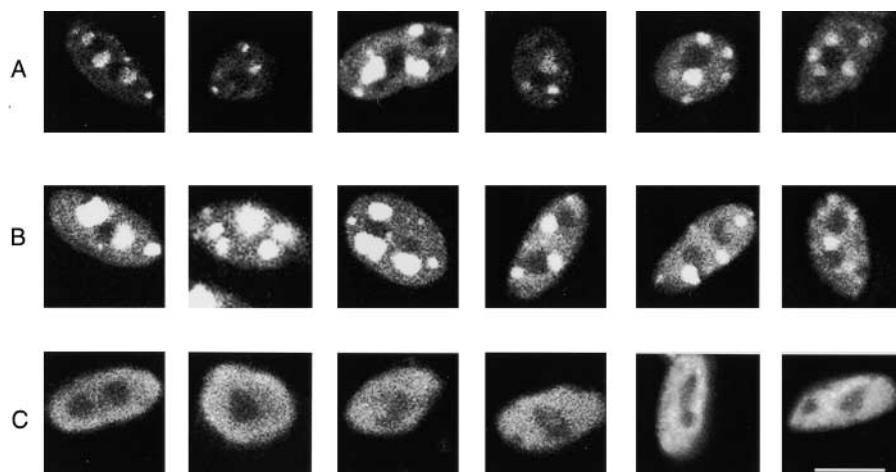
clear distribution of nuclear-targeted NFATc–GFP is not homogenous; instead, it showed a definite punctate pattern of fluorescent foci. Foci were observed in all nuclei of fibers expressing NFATc(S→A)–GFP. The number of foci in each nucleus varied between different nuclei in the same or different fibers.

To exclude the possibility of GFP changing the behavior of NFATc(S→A)–GFP and thus affecting the intranuclear distribution of the NFATc(S→A)–GFP fusion protein, we also analyzed the localization of a FLAG-tagged NFATc(S→A) using immunofluorescence experiments. As shown in Fig. 2 B, we found the anti-FLAG antibody intranuclear staining pattern to be similar to the pattern of intranuclear fluorescent foci in NFATc(S→A)–GFP-expressing fibers. Since FLAG-tagged NFATc lacks the GFP sequence, the nuclear foci cannot be the result of the GFP sequence.

To answer the question of whether this type of focal pattern occurs with other expressed proteins targeted to the nucleus, an adenovirus expressing a  $\beta$ -gal cDNA containing a nuclear-targeting sequence was used as control. 3 d after infection, the fibers were fixed and stained with antibodies. An anti- $\beta$ -gal antibody stain shows a uniform nuclear distribution, with absence of bright foci of nuclear fluorescence. In most of the nuclei there are two round unstained regions, which resemble the two nucleoli in mouse cells (Fig. 2 C). Dark nucleoli are also seen in nuclei of NFATc(S→A)–GFP- or FLAG–NFATc(S→A)-expressing muscle fibers (Fig. 2, A and B, respectively), suggesting that the nuclear NFATc proteins are excluded from nucleolar structures.

### Activity-dependent nuclear translocation

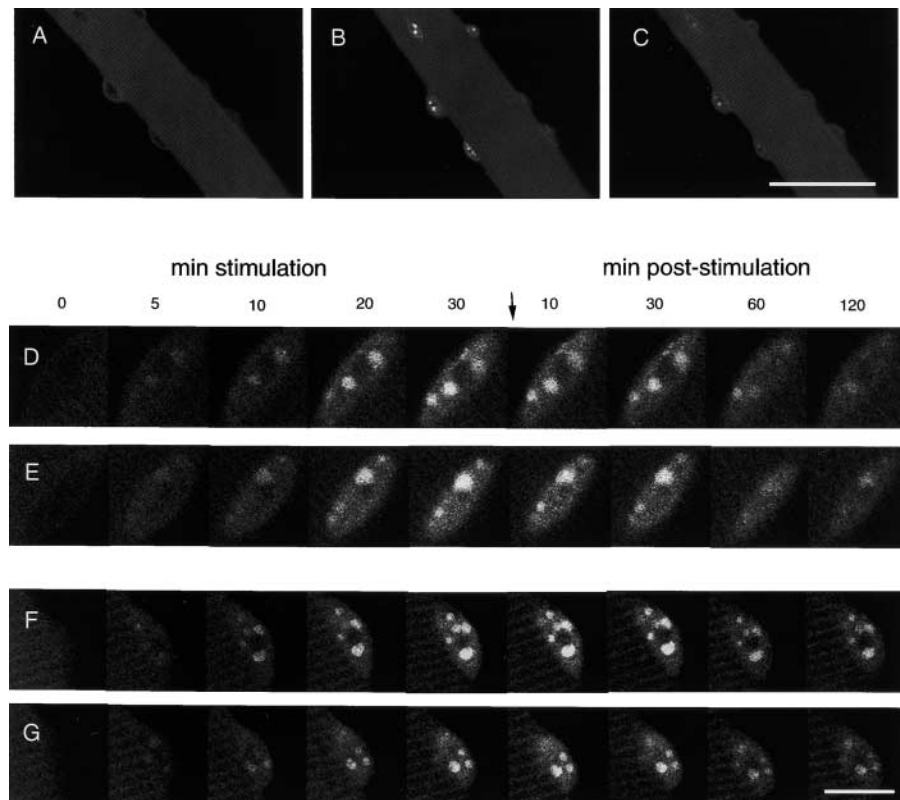
The preceding results establish that constitutively nuclear NFATc(S→A) is localized in multiple distinct intranuclear foci. We next investigated whether the physiological stimulus of fiber electrical activity, and the resulting elevated cytosolic  $[Ca^{2+}]$ , would also result in nuclear translocation and appearance of foci of intranuclear NFATc. Fibers expressing NFATc–GFP were stimulated to produce action potentials using 1 ms pulses of four different patterns: a 10 Hz contin-



**Figure 2. Example nuclei from fibers infected for expression of NFATc or  $\beta$ -gal fusion proteins.** (A) Enlarged images of nuclei of fibers expressing NFATc(S→A)–GFP exhibited a definite pattern of fluorescent foci. (B) Anti-FLAG antibody staining of fibers expressing FLAG–NFATc(S→A) without GFP revealed a similar pattern of nuclear foci, indicating that the nuclear foci were not produced by the GFP. Foci were observed in all nuclei of fibers expressing NFATc(S→A)–GFP or FLAG–NFATc(S→A), and were smaller and more numerous than the nucleoli (darker spots) in each nucleus. (C) Anti- $\beta$ -gal antibody-stained fibers expressing nuclear-targeted  $\beta$ -gal exhibited uniform nuclear fluorescence except for two round unstained regions, presumably corresponding to the

nucleoli. This indicates that the fluorescent foci seen in fibers expressing NFATc(S→A)–GFP were not due to restricted access to various nuclear subdomains. Each row presents six nuclei from three different individual fibers. Bar, 10  $\mu$ m.

**Figure 3. Images of a fiber expressing NFATc-GFP and stimulated with 10-Hz pulses.** A fiber expressing NFATc-GFP is shown before stimulation (A), 30 min after continuous stimulation with 10 Hz pulses (B), and 120 min (C) after cessation of stimulation. After 30 min stimulation (B), the four nuclei in focus exhibit sharp fluorescent foci. The 2 indistinct nuclei at the lower right edge of the fiber are probably in a different focal plane and thus do not exhibit clear intranuclear fluorescent foci. (D-G) Enlarged images of four different nuclei in fibers expressing NFATc-GFP and stimulated with different frequencies. Fibers were stimulated with 10-Hz continuous pulses (D and E) or 10-Hz trains (F and G). Continuous 10-Hz and 10-Hz train stimulation of fibers expressing NFATc-GFP caused fluorescence to appear in intranuclear foci and increase with time in the nuclei. From the earliest fluorescence detection, each nucleus already exhibited a pattern of bright foci that persisted with increasing intensity during continued stimulation lasting up to 30 min. On cessation of stimulation, the nuclear foci were maintained and there was a gradual decline in nuclear fluorescence for 2 h. Time points are labeled, and the time when the stimulation was stopped is denoted. Bars: (A-C) 50  $\mu$ m; (D-G) 10  $\mu$ m.



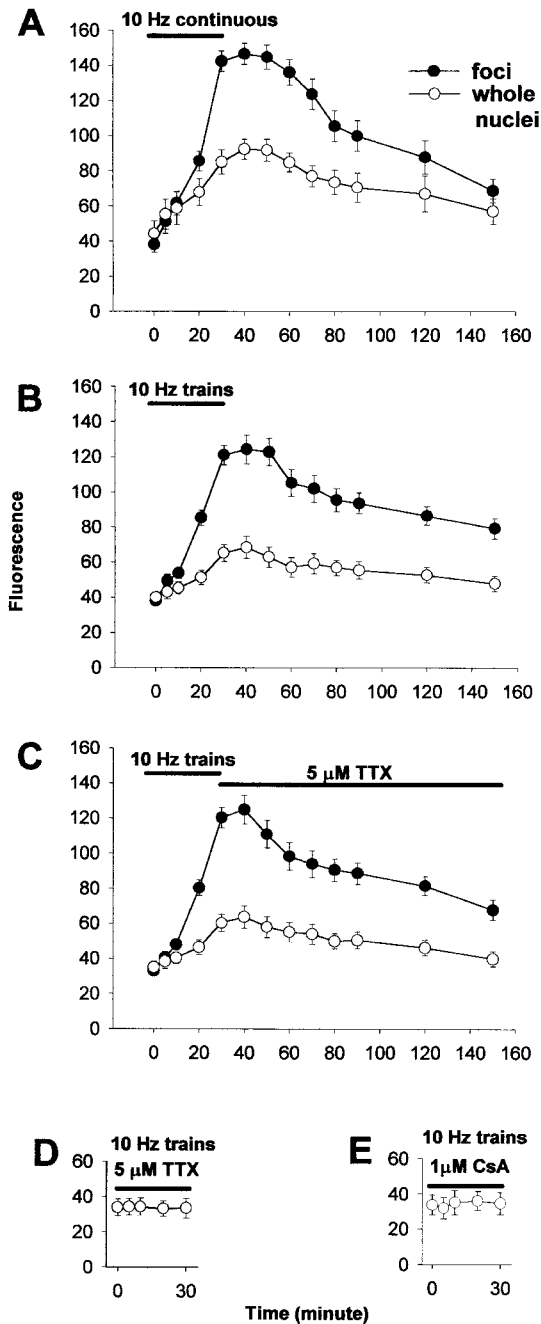
uous stimulation, one 5 s train of 10 Hz stimuli every 50 s, one 0.1 s train of 50 Hz every 50 s, and a 1 Hz continuous stimulation. Field stimulation with any of the four stimulation protocols resulted in visible twitches throughout the period of stimulation in all fibers used for analysis. Fig. 3, A-C, presents images of the same fiber before stimulation (A), 30 min after the start of 10 Hz continuous stimulation (B), and 2 h after cessation of stimulation (C). This electrical stimulation caused a translocation of NFATc into intranuclear foci (B). The disappearance of these fluorescent foci was only partially completed at 2 h after cessation of stimulation (C). In all stimulated fibers expressing NFATc-GFP, intranuclear translocation and the appearance of intranuclear foci was observed in essentially all nuclei present in the focal plane of the image, and in all nuclei appearing in successive z-sections (1- $\mu$ m steps) of a given fiber.

Fig. 3, D-G, present images of four individual nuclei from two different fibers taken at various times during fiber stimulation. One image was taken before the stimulation was started. Images were then taken at 5, 10, 20, and 30 min during stimulation, and then every 10 min during recovery while the fiber was at rest without stimulation (only selected times during recovery are shown in Fig. 3). Continuous 10 Hz stimulation (Fig. 3, D and E) or 5-s trains of 10 Hz stimuli every 50 s (Fig. 3, F and G) both caused NFATc-GFP to translocate from cytoplasm to the nuclei and to be concentrated within intranuclear foci. The first image during stimulation, taken 5 min after stimulation was started, already showed an increase of nuclear fluorescence and a dim but definite pattern of nuclear foci. The intensity of fluorescence in the nuclear foci continuously increased throughout the entire 30-min period of stimulation, and the same pattern of

intranuclear foci was maintained at increasing fluorescence intensity throughout the period of stimulation. Thus, each NFATc focus within the nucleus was gradually accumulating increasing numbers of NFATc molecules throughout the stimulation period. No new foci appeared as nuclear NFATc-GFP accumulated. The intranuclear fluorescence gradually declined after cessation of stimulation, but the pattern of foci was maintained at diminishing overall fluorescence intensity. The increased nuclear fluorescence did not completely reverse by the end of the 2 h observation period after cessation of stimulation.

#### Time course of nuclear translocation of NFATc

To determine whether the stimulation-induced nuclear translocation of NFATc-GFP was frequency dependent, we quantitatively compared the effects of three different frequencies. Continuous 10 Hz stimulation (Fig. 4 A) or 5 s trains of 10 Hz stimuli every 50 s (Fig. 4 B) both resulted in similar nuclear translocation of NFATc-GFP, as judged by the average fluorescence intensity within the nuclear foci (filled circles) or the average fluorescence over entire nuclei (open circles). In both patterns of stimulation, nuclear fluorescence increased continuously during stimulation, remained constant for about 10-20 min after cessation of stimulation, and then began to decrease. The fluorescence of nuclear foci declined to 0.5 of its peak value by 1.3 or 1.9 h ( $= t_{1/2}$ ) after cessation of the continuous 10 Hz stimulation (Fig. 4 A) or the 5 s train of 10-Hz pulses (Fig. 4 B), respectively. Nuclear fluorescence did not decline completely to baseline even by 2 h after cessation of stimulation. In another group of fibers, tetrodotoxin (TTX; 5  $\mu$ M) was applied to the fiber at the termination of a 30-min stimulation



**Figure 4. Time course of nuclear translocation of NFATc.** The average fluorescent intensity per pixel over whole nuclei (open circles) or over the intranuclear foci (filled circles) was quantitated as described in Materials and methods. Continuous 10 Hz stimulation (A) or 5-s trains of 10 Hz stimuli every 50 s (B and C) all resulted in similar nuclear translocation of NFATc-GFP. In all three cases, nuclear fluorescence increased continuously during the 30-min stimulation period, remained constant for about 10–20 min after cessation of stimulation, and then began to decrease. Nuclear fluorescence was still above the baseline value 2 h after stimulation was stopped. In C, 5  $\mu$ M TTX was added immediately after the 10-Hz train stimulation was stopped. In D and E, fibers were incubated with 5  $\mu$ M TTX or 1  $\mu$ M CsA, respectively, for 30 min before the 10-Hz train stimulation was started (the TTX or CsA was present in the Ringer's solution throughout the experiment). Stimulation with 10-Hz trains did not cause any change in nuclear fluorescence in the presence of 5  $\mu$ M TTX (D) or 1  $\mu$ M CsA (E). Results are expressed as the mean  $\pm$  SE. (A) 25 foci of 11 nuclei from 5 fibers; (B) 34 foci of 14 nuclei from 6 fiber; (C) 25 foci of 8 nuclei from 5 fibers; (D) 11 nuclei from 5 fibers; (E) 9 nuclei from 5 fibers.

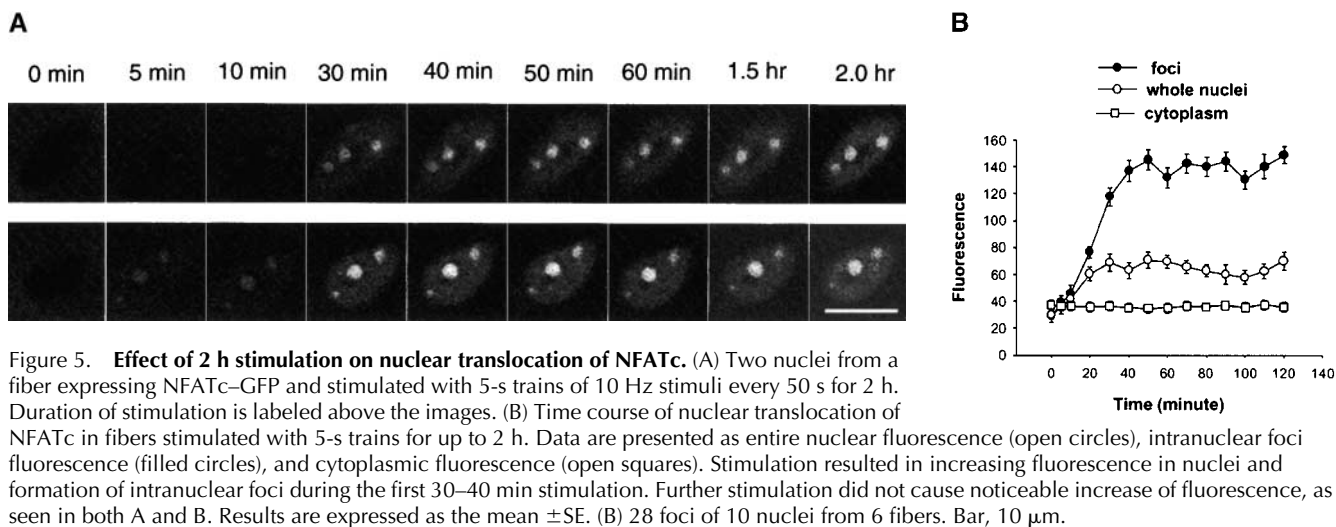
with 10-Hz trains. In the presence of TTX, the decay of nuclear fluorescence ( $t_{1/2} = 1.6$  hr) was similar to that without TTX (compare Fig. 4, C and B), indicating that possible fiber-spontaneous electrical activity after cessation of electrical stimulation did not influence the loss of previously translocated NFATc from the nucleus. No spontaneous fibrillation of the fibers was seen during observation of the fibers either before or after stimulation in the present experiments, as previously observed under similar culture conditions of unstimulated adult FDB fibers (Bekoff and Betz, 1977).

In the presence of 5  $\mu$ M TTX, no nuclear translocation of NFATc-GFP was observed during stimulation using 10-Hz trains (Fig. 4 D), ruling out a possible direct effect of electric current on NFATc localization. The calcineurin inhibitor CsA (1  $\mu$ M) also completely prevented nuclear translocation of NFATc-GFP (Fig. 4 E), indicating an essential role for calcineurin in the nuclear translocation of NFATc during electrical stimulation of adult skeletal muscle fibers, as during  $K^+$  depolarization of neurons (Graef et al., 1999) or during  $Ca^{2+}$  activation of T-lymphocytes (Timmerman et al., 1996).

Using 5-s trains of 10 Hz stimuli every 50 s, prolonging the period of stimulation from 30 min to 2 h caused only a moderate further increase in the fluorescence of nuclear foci and of the entire nuclei during the period between 30 min and 1 h, after which fluorescence remained constant during the second hour of stimulation (Fig. 5 A). Since cytosolic NFATc fluorescence did not decline during the entire period of stimulation (Fig. 5 B), the nuclear translocation of NFATc represents a small fraction of the total amount of NFATc-GFP expressed in a given muscle fiber. Thus, the steady nuclear fluorescence during the second hour of stimulation does not reflect a depletion of the pool of NFATc available for nuclear translocation. Assuming that NFATc can leave the nucleus at a similar rate both during and after stimulation, the steady nuclear content during the second hour of stimulation would reflect a balance between constant rates of nuclear uptake and nuclear loss of NFATc. The steady level of fluorescence of the intranuclear NFATc foci during continued stimulation is unlikely to reflect saturation of NFATc binding sites within the foci since the intensity of the foci in fibers expressing NFATc(S $\rightarrow$ A)-GFP was roughly an order of magnitude higher than in stimulated fibers expressing NFATc-GFP. As in the case of the 30-min stimulation experiments, the pattern of intranuclear foci remained constant throughout the entire 2-h stimulation period, even though the intensity of the pattern increased during the first hour of stimulation.

### The stimulation pattern influences nuclear translocation of NFATc

In stark contrast to the effect of the 10 Hz stimulation, 1 Hz continuous stimulation, which gives the same average rate of pulses per minute as 5-s trains of 10 Hz stimuli every 50 s, did not induce any change in nuclear fluorescence intensity (Figs. 6, A and B, and 7 A), even though fiber contraction in response to stimulation was observed throughout the period of stimulation. Thus, the nuclear translocation of NFATc is strongly dependent on the temporal pattern in which the stimuli are applied, and not just on the overall average fre-

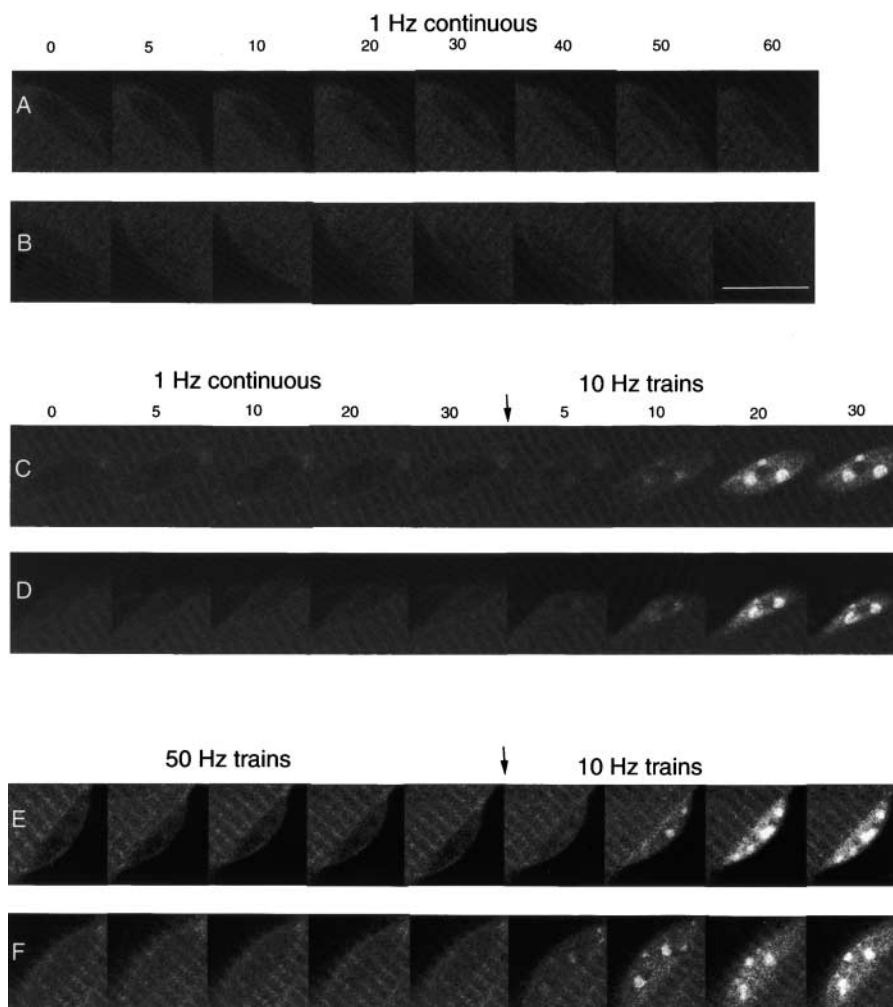


quency of stimulation. Fig. 7 A presents only whole nuclear fluorescence data, since there was no translocation of NFATc to the nucleus, and thus no nuclear foci formed.

After 30 min of 1 Hz continuous stimulation, which caused no increase in nuclear fluorescence, changing to stimulation

with 10-Hz trains caused the appearance of foci of intranuclear fluorescence (Figs. 6, C and D, and 7 B). The same fibers that did not respond to continuous stimulation at 1 Hz were thus capable of producing a normal response to subsequent stimulation with 10-Hz trains of pulses (compare Fig. 7 B with 4 B).

**Figure 6. Enlarged images of six nuclei from three different fibers expressing NFATc-GFP and stimulated with different frequencies.** (A and B) A fiber was stimulated with 1-Hz pulses for 1 h. (C and D) A fiber was first stimulated with 1 Hz for 30 min, and then the same fiber was stimulated with 10-Hz trains for another 30 min. (E and F) A fiber was first stimulated with 50-Hz trains for 30 min, and then the same fiber was stimulated with 10-Hz trains for another 30 min. Frequencies and time points are labeled, and the time when the stimulation frequency was switched is denoted. Bars, 10  $\mu$ m.



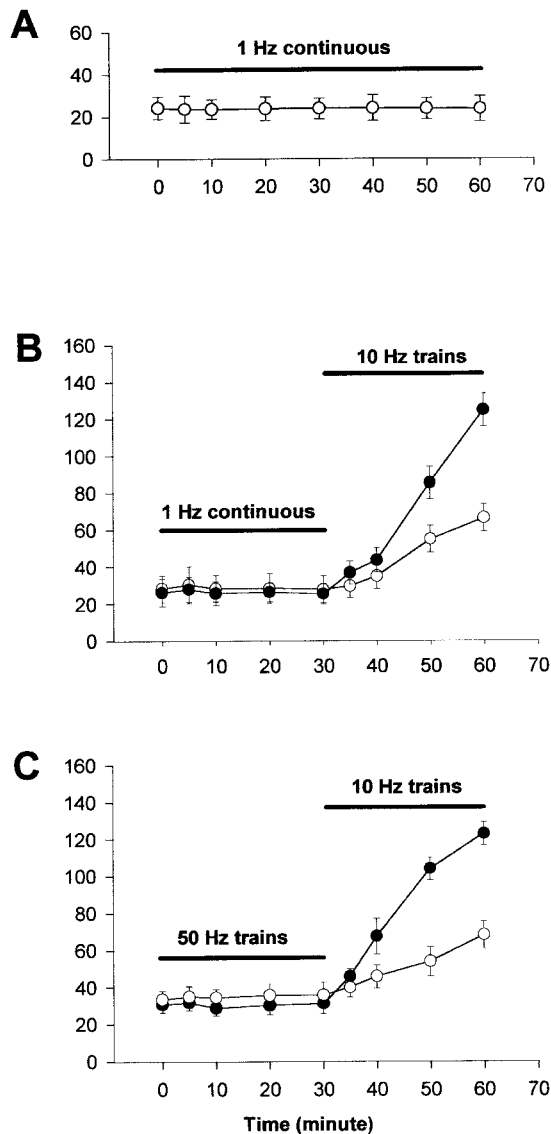


**Figure 7. 1 Hz stimulation does not cause nuclear translocation of NFATc.** (A) Continuous stimulation at 1 Hz up to 1 h caused no detectable changes in nuclear fluorescence. (B and C) Fibers were first stimulated with 1-Hz pulses (B) or 50-Hz pulses of 0.1 s duration every 50 s (C) for 30 min, then the stimulation frequencies were switched to 10-Hz trains. Although 1 Hz continuous stimulation (B) or 50-Hz trains (C) resulted in no detectable change in nuclear fluorescence, subsequent stimulation using 10-Hz trains caused significant increases in whole nuclear fluorescence and resulted in appearance of nuclear foci in the same group of fibers. (A) 20 nuclei from 8 fibers; (B) 18 foci of 8 nuclei from 5 fibers; (C) 17 foci of 9 nuclei from 5 fibers.

Stimulation of fibers with a fast-twitch muscle fiber pattern of activity (50 Hz for 0.1 s every 50 s), also did not induce nuclear translocation. In the same fibers, subsequent stimulation with 10-Hz trains resulted in nuclear translocation and appearance of intranuclear fluorescent foci (Figs. 6, E and F, and 7 C).

### Pharmacological activation of nuclear translocation of NFATc

Since nuclear translocation of NFATc during electrical stimulation requires dephosphorylation by calcineurin (Fig. 4 E),

we examined whether pharmacological perturbation of the balance between kinases and phosphatases would influence NFATc localization in the absence of electrical stimulation. Addition of the kinase inhibitors 20  $\mu$ M PD98059 and 30  $\mu$ M SB202190 (Fig. 8 B) or 5 mM LiCl (Fig. 8 B) resulted in nuclear translocation of NFATc and the formation of intranuclear fluorescent foci similar to those resulting from electrical stimulation. Fibers incubated for the same period of time, but in the absence of pharmacological agents, exhibited negligible nuclear translocation (Fig. 8 C). Finally, presumed elevation of cytosolic  $[Ca^{2+}]$  by exposure of fibers to ionomycin (1  $\mu$ M) also resulted in nuclear translocation of NFATc and appearance of intranuclear fluorescent foci (unpublished data).

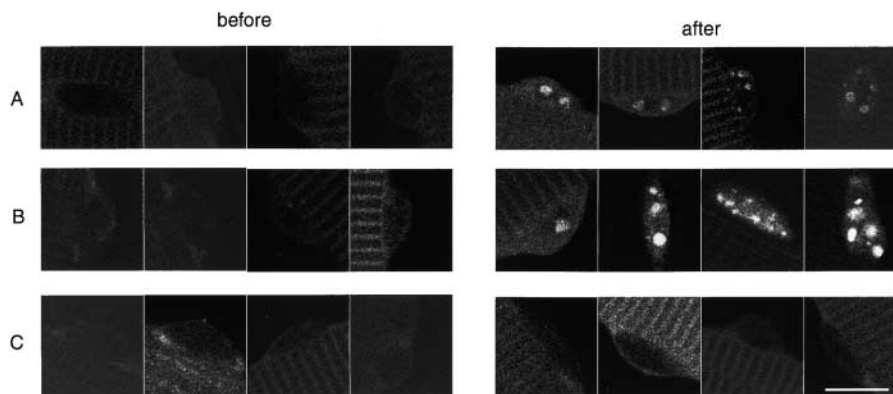
### Organization and nature of NFATc nuclear foci

Fig. 9 shows optical sections of two nuclei from two different muscle fibers taken at successive 1- $\mu$ m focal planes. Both fibers were infected with adenovirus-containing NFATc-GFP and stimulated with 10-Hz pulses for 30 min before recording the z axis sections shown in Fig. 9. These z-sections reveal that foci were distributed inside the nuclei, some close to the edge of the nuclei, and some deep inside. The foci exhibited a range of diameters, even in the same nucleus. Foci diameters ranged from  $<0.5 \mu$ m (arrowheads) to  $>2 \mu$ m (arrows). The largest foci are visible in several successive optical sections of each nucleus, consistent with the z resolution for the confocal microscope used in this experiment of about 1.0  $\mu$ m and the  $>2\text{-}\mu$ m diameter of the largest foci. In contrast, the smallest foci were generally visible only in at most two neighboring optical sections. Fig. 9 also shows that the largest foci exhibit signs of substructure within the focus. Based on serial images of 13 nuclei, the number of clearly resolvable fluorescent foci per nucleus varied between 4 and 9. There was no apparent difference in number of intranuclear foci between stimulated fibers expressing NFATc-GFP and nonstimulated fibers expressing NFATc(S $\rightarrow$ A)-GFP or FLAG-NFATc(S $\rightarrow$ A).

The splicing factor SC-35 and the transcription factor myocyte enhancer factor 2 (MEF2) have both been previously shown to exhibit nonuniform intranuclear distributions (Spector et al., 1991; Miska et al., 1999; Smith et al., 1999). Staining of NFATc(S $\rightarrow$ A)-GFP-expressing muscle fibers with primary antibodies to either SC-35 or to MEF2, followed by Texas red secondary antibody staining, revealed that both SC-35 and MEF2 exhibited nonuniform intranuclear distributions in cultured adult skeletal muscle fibers, but that neither of these molecules colocalized with intranuclear NFATc-GFP (Fig. 10). Thus, the foci do not appear to be general, nonspecific storage depots for splicing or transcription factors within the nucleus. The nature and function of the intranuclear foci containing NFATc remains to be determined. Interestingly, comparison of the intranuclear distributions of NFATc and SC-35 or MEF2 in Fig. 10 indicates that NFATc is concentrated in foci immediately adjacent to, but not overlapping the nucleoli (dark in Fig. 10), and that both SC-35 and MEF2 appear to be excluded from the NFATc foci.

**Figure 8. Kinase inhibitors cause nuclear translocation of NFATc-GFP and formation of nuclear foci.** FDB fibers were infected with NFATc-GFP. (A)

Enlarged nuclear images from a group of fibers, before or after 20  $\mu$ M PD 98059 and 30  $\mu$ M SB 202190 were added and incubated for another 2 h. (B) Fibers were treated with LiCl (5 mM) for 2 h. (C) Control fibers, without any kinase inhibitors added, have no nuclear translocation of NFATc-GFP. The pattern of nuclear foci, the result of kinase inhibitors, was similar to the foci caused by proper frequency of electrical stimulation.



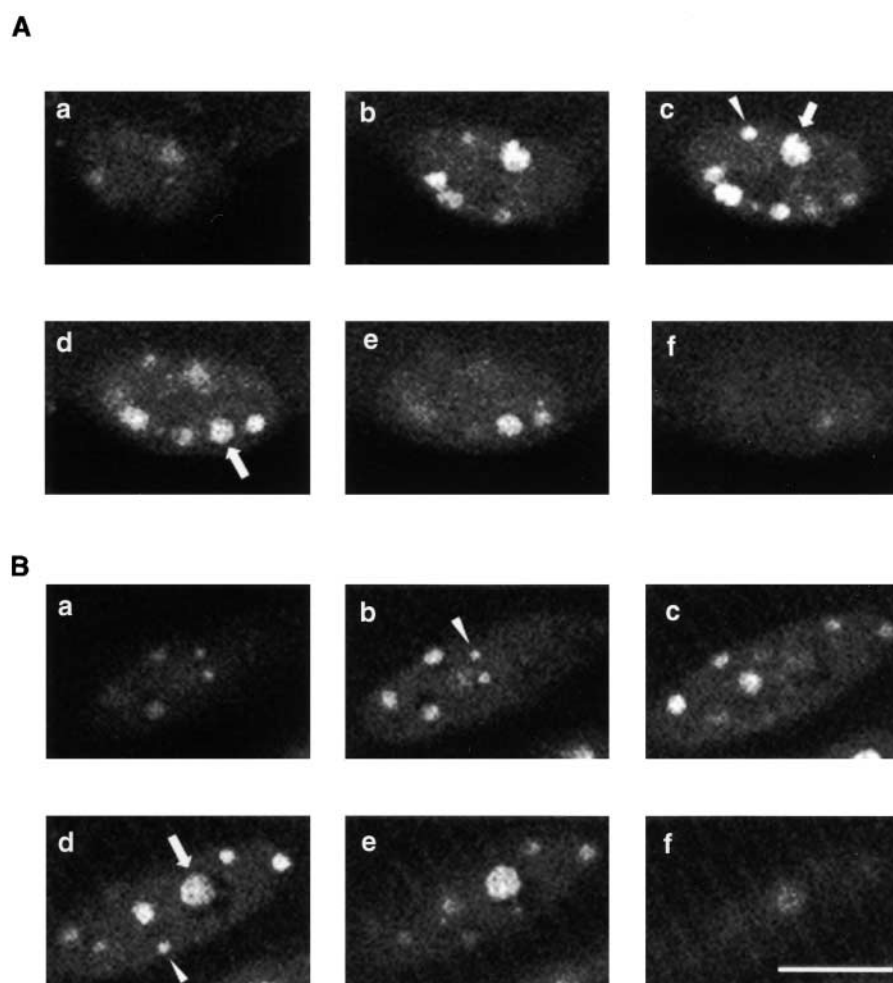
## Discussion

This report represents the first study of the movement and intranuclear location of the transcription factor NFATc in isolated adult skeletal muscle fibers. In contrast to previous studies, we here used fully mature adult skeletal muscle fibers instead of dividing muscle cell lines, myoblasts, or myotubes. We used physiological action potential activation of these fibers, which causes physiological calcium transients, instead of using sarcoplasmic reticulum ATPase inhibitors or calcium ionophores to elevate myoplasmic

[Ca<sup>2+</sup>], which results in steady increases of resting calcium. Using this approach, we now report three novel findings regarding the movement and localization of the transcription factor NFATc in adult skeletal muscle fibers. (a) NFATc translocation into nuclei is activity pattern-dependent in adult skeletal muscle fibers. NFATc translocates to muscle nuclei in response to repeated trains of 10 Hz stimuli but not in response to continuous 1 Hz stimulation, both of which provide the same mean frequency of stimulation averaged over minutes of stimulation. (b) NFATc exhibits a nonuniform nuclear distribution with intranu-

**Figure 9. Z-section images of two nuclei from two different living fibers expressing NFATc-GFP, and stimulated for 30 min with 10-Hz pulses continuously.** Images a-f in both A and B correspond to successive 1- $\mu$ m thick sections separated by 1- $\mu$ m steps in the z-direction. Foci diameters ranged from sub- $\mu$ m to >2  $\mu$ m, as denoted with arrowhead or arrow, respectively.

Bar, 10  $\mu$ m.





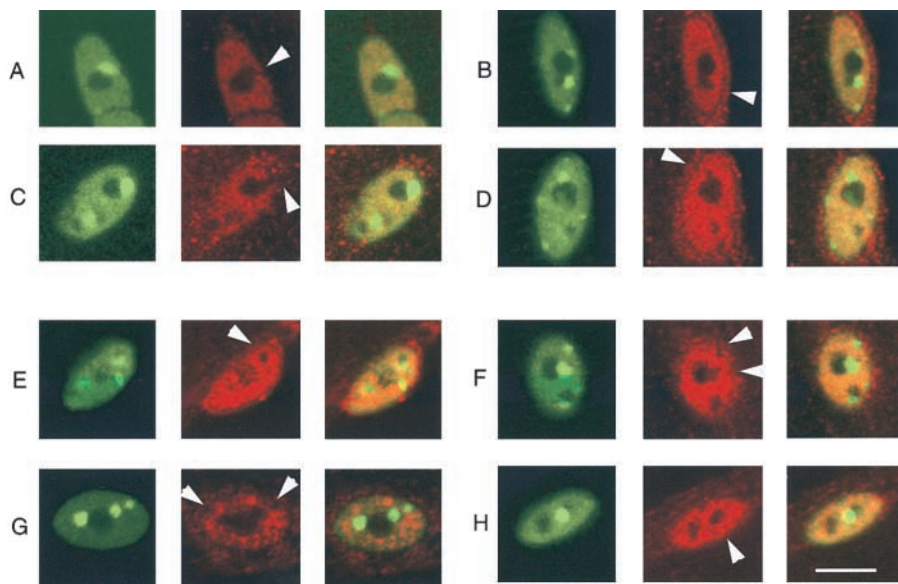


Figure 10. **MEF2 and SC-35 do not colocalize with NFATc in nuclei.** (A–D) Enlarged images of four different nuclei from different fibers, which expressed NFATc(S→A)–GFP and immunostained for MEF2. (E–H) Images of four nuclei from different fibers expressing NFATc(S→A)–GFP, and immunostained for SC-35. Shown are NFATc nuclear foci as green (left), MEF2 or SC-35 as red (center), and overlay (right). Arrowheads denote images of NFATc(S→A)–GFP fluorescent foci that lack staining for MEF2 (A–D) or SC-35 (E–H).

clear foci of concentration. (c) Accumulation of NFATc in intranuclear foci increases during the first hour of appropriate stimulation, and declines during the subsequent hours after cessation of stimulation, but the pattern and intranuclear location and the number of the foci remains constant during these changes in intensity.

#### Calcineurin/NFATc and skeletal muscle

NFAT is a transcription factor originally found to be involved in T cell signaling (for review see Rao et al., 1997; Crabtree, 1999). Endogenous NFAT requires calcineurin activity to translocate to the nucleus to modulate gene expression. In the inactive state, NFAT resides in the cytosol in a phosphorylated form, but translocates to the nucleus upon dephosphorylation. This is accomplished by the  $\text{Ca}^{2+}$ -dependent phosphatase calcineurin that binds and dephosphorylates NFAT (Beals et al., 1997) at a serine-rich region (SRR) containing two partially redundant nuclear localization signals close to its  $\text{NH}_2$ -terminal (Luo et al., 1996). An NFATc construct bearing S→A mutants, which has all 11 serines replaced with alanines in the SRR, as used in our experiments, is constitutively localized to the nucleus independent of calcium stimulation (Beals et al., 1997). Five NFAT isoforms have been identified so far, with isoform NFATc being the predominant one expressed in skeletal muscle (Hoey et al., 1995).

Recently, it was reported by several laboratories that calcineurin/NFAT regulates skeletal muscle differentiation and fiber type-specific gene expression in myogenic cell lines and primary myotube cultures (Abbott et al., 1998; Delling et al., 2000; Friday et al., 2000). Although three isoforms of NFAT are expressed in the cytoplasm of muscle cells at different stages of myogenesis, each isoform undergoes calcium-induced cytoplasm to nuclear translocation at specific stages of muscle differentiation (Abbott et al., 1998). In multinucleated myotubes, which is the stage of muscle differentiation closest to adult muscle, NFATc (NFATc1 or NFAT2) responds to a thapsigargin-induced elevation of cytosolic calcium by translocating to nuclei from cytoplasm.

In predifferentiated C2C12 myoblasts, NFATc3, but not NFATc, translocated to nuclei in response to activated calcineurin (Delling et al., 2000). Using Northern blot analyses Hoey et al. (1995) found that NFATc was strongly transcribed in adult human skeletal muscle. Chin et al. (1998) proposed that the calcineurin–NFATc pathway is important for slow fiber type-specific gene expression. Treatment of rats for 6 wk with CsA, a specific calcineurin inhibitor, increased the number of histochemically detectable fast twitch fibers within the soleus muscle (Chin et al., 1998). Promoter analysis demonstrated that calcineurin-stimulated transactivation of slow fiber-specific genes requires nucleotide sequence motifs characteristic of NFATc binding sites (Chin et al., 1998).

The majority of studies in the above reports (Abbott et al., 1998; Chin et al., 1998; Delling et al., 2000) used immature, embryonic-like myotubes or cultured cell lines. We now show that NFATc is exclusively cytoplasmic in unstimulated adult skeletal muscle fibers in cultures and is localized to the z-line of the sarcomere. The z-line localization of NFATc in resting fibers is consistent with the recent report that calcineurin localizes to the z-line in skeletal muscle via the binding protein calsarcin (Frey et al., 2000), and the report that in resting cells NFAT docks on calcineurin (Garcia-Cozar et al., 1998).

Relatively little is known concerning the behavior of NFATc in mature muscle fibers in response to muscle fiber electrical stimulation. The effect of different frequencies of stimulation in single adult fibers, even at the single nucleus level, has not been investigated previously. Cellular calcium is believed to play a key role in fiber type transformation (Kubis et al., 1997). It has been proposed that a tonic firing pattern, typical of motoneuron activity innervating slow-twitch muscle, results in maintained elevation of cytosolic calcium, and activation of NFATc (Chin et al., 1998). Slow-twitch skeletal muscle (soleus) has higher resting calcium than fast-twitch muscle (FDB) (Carroll et al., 1997, 1999), and chronic stimulation of fast-twitch muscle increases the resting calcium to the range characteristic of slow-twitch

muscle (Carroll et al., 1999). However, the down-stream signal transduction pathway has not been established. One question is how the different frequencies of cellular calcium transients are sensed and decoded by the cell. The calcineurin/NFATc pathway is one of the suggested candidates. Our results now show that NFATc is cytoplasmic in unstimulated, fast-twitch, adult murine skeletal muscle fibers. The cytoplasmic NFATc responds to 10 Hz continuous stimulation and to 10-Hz trains by translocating to the nucleus, but exhibits negligible translocation to the nucleus during 1 Hz continuous stimulation. Nuclear translocation of NFATc also did not occur in response to the fast-twitch fiber type stimulation pattern of 50 Hz for 0.1 s every 50 s. Thus, translocation of NFATc in response to electrical activity appears to require a stimulation pattern similar to slow fiber type activity. The nuclear translocation of NFATc in response to electrical stimulation involves activation of calcineurin and subsequent dephosphorylation of NFATc by calcineurin since it is blocked by the calcineurin inhibitor CsA. Furthermore, nuclear translocation of NFATc in these muscle fibers can be pharmacologically produced by kinase inhibitors, indicating a balance between dephosphorylation and phosphorylation in NFATc translocation.

#### Stimulation pattern-dependent nuclear translocation

The observed dichotomy between the absence of nuclear accumulation of NFATc during a continuous 1 Hz stimulation, and its marked nuclear accumulation during stimulation with 5-s bursts of 10-Hz pulses repeated every 50 s, was quite striking. It was all the more remarkable because the mean frequency of stimulation, averaged over minutes of stimulation, was actually the same 1-Hz mean rate in both cases. By following the decay of nuclear fluorescence after 30 min of stimulation with the 10-Hz train or continuous pattern, the half time of decay of nuclear fluorescence was found to be  $\sim 1.5$  h. With this half time, only a very small fraction of the NFATc in the nucleus at the end of any 10-Hz train would leave the nucleus during the subsequent 45 s before the start of the next train. We were unable to determine the rate of loss of nuclear NFATc after 1 Hz stimulation, since nuclear accumulation of NFATc did not occur in that case. However, if the half time of loss of nuclear NFATc during 1 Hz stimulation were the same as after the 10-Hz trains, even a smaller proportion of nuclear NFATc would have left the nucleus between successive pulses in the 1 Hz stimulation. Therefore, either negligible NFATc entered the nucleus during the 1 Hz stimulation, or the loss of NFATc from the nucleus must have exhibited a much longer half time after the 10-Hz trains than after the 1 Hz stimuli. Although modulation of nuclear exit of NFATc by calcineurin-dependent processes has some precedent (Hogan and Rao, 1999; Zhu and McKeon, 1999), it seems more likely that the primary regulation of nuclear NFATc is at the entry steps.

The question of how a set number of action potentials grouped together in a 10-Hz train produced nuclear entry of NFATc, while the identical number of action potentials given at a continuous 1-Hz rate did not, may be partly answered by the issue of positive cooperativity. In that case the responses to two closely spaced stimuli would positively in-

teract so that the response to the two stimuli would be considerably greater than the sum of the two separate responses. In the path to the nuclear build up of NFATc, cooperativity could be involved at one or more of the following steps:  $\text{Ca}^{2+}$  elevation, calcineurin activation, NFATc dephosphorylation, and NFATc translocation into the nucleus. In fact, positively cooperative aspects of each of these steps could contribute to an overall apparent cooperative effect that is greater than that of any of the individual steps in the sequence. Thus, positively cooperative aspects of the individual steps may have been reinforced and amplified by the sequential activation path, resulting in the observed dichotomy between the responses for these two patterns of applying the same number of stimuli.

In the steady state during repeated trains of 10 Hz stimulation, the small loss of NFATc from the nucleus between trains (above) must be just balanced by a small influx per train, giving an average steady level of nuclear NFATc. A small nuclear influx of NFATc per train would account for the need to use about 30–60 min of stimulation with the 10-Hz trains pattern (i.e.,  $>30$ –60 trains of pulses) to attain a steady state of nuclear NFATc in our experiments using repeated trains of 10 Hz stimulation. The relatively slow loss of NFATc from the nucleus of FDB fibers after stimulations is in contrast to the situation in lymphocytes, where a sustained (Timmerman et al., 1996; Dolmetsch et al., 1997) elevation of intracellular calcium was required to maintain NFATc in the nucleus. The slow loss of NFATc from nuclei in the present muscle fiber experiments is even slower than the relatively slow loss of NFATc from nuclei of hippocampal neurons after neuronal stimulation to elevate cytosolic  $[\text{Ca}^{2+}]$  (Graef et al., 1999).

#### Substructure of the nucleus: transcription factor domains in nucleus

It has been long known that eukaryotic nuclei are not homogeneous but contain a variety of subnuclear structures, often referred to as nuclear bodies. Most of them are involved in the synthesis, processing, and modification of RNA (Lamond and Earnshaw, 1998; Lewis and Tollervey, 2000; Misteli, 2001). In the nucleus, individual chromosomes occupy discrete regions and are separated by inter-chromosomal domains. A nonuniform distribution inside the nucleus of constructs of components of the transcriptional machinery has been reported either using GFP tag, FLAG tag, or immunohistochemical staining (Ktistaki et al., 1995; Htun et al., 1996; Fejes-Toth et al., 1998). However, the significance of the distribution in these subnuclear domains remains uncertain.

We now present the first report that NFATc is also localized in subnuclear domains when present in the nucleus. Previous studies of NFAT nuclear translocation have not noted the concentration of NFAT into discrete subnuclear domains. NFAT appeared to be uniformly distributed within the nucleus in the figures of previous publications on either cultured muscle cells (Figs. 4 and 6 in Abbott et al., 1998; Fig. 3 in Delling et al., 2000) or neurons (Fig. 3 in Graef et al., 1999). Furthermore, we have not found any report or any indications of a similar nuclear distribution of NFATc as found in this report. It is unlikely that viral proteins expressed by the adenovirus vector modified the nu-

clear distribution, since we found a uniform distribution of virally delivered, nuclear-targeted  $\beta$ -galactosidase. Likewise, spatial restriction because of the molecular mass or the nature of nuclear location signal are not likely reasons for the different nuclear distribution patterns of  $\beta$ -gal and NFATc-GFP, since the molecular weight of a  $\beta$ -gal tetramer ( $4 \times 116$  kD; Fowler and Zabin, 1977) would be much greater than NFATc-GFP fusion ( $\sim 35$  kD) used in our experiments, and both proteins use similar nuclear location signal (Kalderon et al., 1984; Beals et al., 1997). The four to nine NFATc foci per nucleus observed here in electrically stimulated muscle fibers are much less numerous than the clusters of mineralocorticoid receptors observed in hormonally activated cells (Fejes-Toth et al., 1998). We have also shown that neither the general splicing factor SC-35, nor the transcription factor MEF2 are colocalized with NFATc in the intranuclear foci. In fact, both SC-35 and MEF2 appear to be excluded from the NFATc foci. Since both NFATc and MEF2 are thought to act together to activate expression of slow fiber type genes (Wu et al., 2000), it is therefore unlikely that the NFATc foci described here are the locations of the slow fiber genes within the nucleus. Rather, the foci may be sites of NFATc storage within the nucleus, consistent with our observation that each focus can accommodate an increasing number of molecules of NFATc during prolonged stimulation.

In conclusion, our results indicate that in skeletal muscle, NFATc translocates from the cytosol to the nucleus in response to electrical stimulation, and that within the nucleus NFATc is concentrated in discrete intranuclear foci. Translocation of NFATc occurred in response to repeated trains of 10 Hz stimuli, but not in response to continuous 1 Hz stimulation, both of which provided the same mean frequency of stimulation averaged over minutes of stimulation. Thus, the translocation of NFATc from cytosol to nucleus is highly activity pattern-dependent in adult skeletal muscle fibers.

## Materials and methods

### Construction of recombinant adenoviruses

The expression construct of NFATc and the NFATc construct with SRR mutations were gifts from Dr. G.R. Crabtree (Howard Hughes Medical Institute, Stanford, CA) (Beals et al., 1997). These two constructs have the FLAG epitope tag 5' to the second codon of the human NFATc cDNA. The plasmids of NFATc-GFP fusion proteins were constructed in pEGFP-N1 (CLONTECH Laboratories, Inc.), with the replacement of the native stop codon of NFATc by a seven amino acid insertion preceding the EGFP coding sequence. A schematic of the NFATc-GFP fusions is shown as Fig. 1, A and B. Recombinant adenovirus (Ad5) containing NFATc or NFATc-GFP cDNA, driven by the cytomegalovirus promoter, were produced according to the methods of Hardy et al. (1997). The NFATc cDNAs were subcloned into the shuttle plasmid pAdlox. These were then subsequently cotransfected with the adenoviral DNA partner,  $\psi 5$ , into an HEK 293 stable cell line expressing cre recombinase (CRE8) and incubated in medium (DME containing 10% heat-inactivated fetal bovine serum, 100 U/ml penicillin, 100  $\mu$ g/ml streptomycin, and 0.8 mg/ml G418). The recombinant products were selected by repeated passage in CRE8 cells. The recombinant adenovirus stocks were purified by ultra centrifugation using cesium chloride density gradients (Graham and Prevec, 1995). The titers were determined from  $A_{260}$  with 1.0 absorbance unit being equivalent to  $\sim 10^{12}$  particles/ml.

The recombinant adenovirus of nuclear-targeted  $\beta$ -gal was a gift from Dr. Yumi Kanegae (Lab of Molecular Genetics, Institute of Medical Science, University of Tokyo, Japan) (Kanegae et al., 1995; Miyake et al., 1996). Nuclear-targeted  $\beta$ -gal was used as a control for the pattern of nuclear localization of NFATc. It has no sequence homology with any of the three NFATc constructs we used here.

### Infection of recombinant adenoviruses in FDB fibers

Single muscle fibers were enzymatically dissociated from FDB muscles of 4–5-wk-old CD-1 mice and cultured as described previously (Liu et al., 1997). In brief, the muscles were incubated with 5 ml MEM (GIBCO BRL) with 10% fetal bovine serum (Biofluid) containing 0.2% collagenase (type I; Sigma-Aldrich) for 3 h. The muscles were teased and triturated to release single fibers. Single fibers were cultured in 35-mm plastic petri dishes with a 10-mm diameter hole through the center and a glass coverslip glued to the bottom. The glass coverslip was coated with laminin (Sigma-Aldrich) before fiber plating. The muscle fibers were cultured with MEM containing 10% fetal bovine serum and 50  $\mu$ g/ml gentamicin sulfate in 5%  $\text{CO}_2$  (37°C). The virus infection ( $7 \times 10^{11}$  particles/ml) was done about 20 h after the fibers were plated on dishes. Before infection, the FDB cultures were rinsed twice with MEM without serum. The recombinant adenoviruses were added to the culture dishes with MEM without serum. The cultures were kept in the  $\text{CO}_2$  incubator for 1 h and the medium was then changed to virus-free MEM with fetal bovine serum and gentamicin for continuous culture.

### Microscopy and image analysis of translocation of NFATc in living fibers

Approximately 72–76 h after infection, culture medium was changed to Ringer's solution, consisting of (in mM) 135 NaCl, 4 KCl, 1  $\text{MgCl}_2$ , 10 Hepes, 10 glucose, and 1.8  $\text{CaCl}_2$ , pH 7.4). The culture chamber was mounted on an inverted microscope (IX70; Olympus) equipped with a confocal laser scanning imaging system (MRC-600; Bio-Rad Laboratories). This system utilizes an argon ion laser which supplies excitation wavelength of 488 nm. Fibers were viewed with an Olympus 60 $\times$ /1.4 NA water immersion objective. The fiber culture chamber was placed on the stage and studied at room temperature. All fibers were scanned at 1.6 $\times$  zoom using constant laser power and gain. Each confocal fluorescence image represents an individual optical section. Axial (z) resolution for the confocal pinhole setting used in this experiment was calibrated previously as  $\sim 1.0$   $\mu$ m (Lacampagne et al., 1996). Two platinum electrodes connected to a stimulator were placed into the fiber culture chamber to give field stimulation. Before the fiber was given any stimulation, one image was taken as control and the focus was adjusted to obtain a sharp view of one or more nuclei. Four stimulation protocols were used: 10 Hz continuously, a 5 s train of 10 Hz stimuli once every 50 s, 1-Hz continuously, and a 0.1 s train of 50 Hz stimuli every 50 s. The duration of the stimulating pulse was 1 ms in all protocols. Pulse polarity was reversed after every pulse to avoid polarization effects. The stimulation voltage was 15–30 V, adjusted to give microscopically observed fiber contraction in all cases. Most fibers remained attached to the laminin-coated coverslip throughout the period of fiber stimulation and recovery, and only such fibers were used to obtain the data reported here. However, the strength and pattern of the mechanical attachment of the fiber to the substrate, and the consequent mechanical effects of fiber stimulation on fiber loading, may have varied considerably from fiber to fiber. Confocal images were taken sequentially after the stimulation was started. In one protocol, images were taken at 5, 10, 20, and 30 min, after which the stimulation was stopped and the fiber was observed for 120 min with images taken every 10 min to record the translocation of NFATc after the stimulation.

The areas of interest (AOI) in each image were quantitated using software custom-written in the IDL programming language (Research Systems). With this program we can obtain the average pixel value of each AOI, which is proportional to the average intensity of fluorescence within the AOI.

### Indirect immunofluorescence histochemistry

FDB cultures infected with adenovirus containing NFATc(S $\rightarrow$ A) or nuclear-targeted  $\beta$ -gal cDNA were fixed with 4% paraformaldehyde at room temperature for 10 min and rinsed three times with PBS. The fibers were then permeabilized with 1% Triton X-100 for 20 min at room temperature. Nonspecific binding sites were blocked by incubation with 2% goat serum. Subsequently, the fibers were incubated for 24 h at 4°C with monoclonal antibodies either against FLAG (M2; Sigma-Aldrich) or against  $\beta$ -gal (Sigma-Aldrich). Both antibodies were diluted 1:500 in 2% goat serum. After washing in four changes of PBS, the fibers were incubated in secondary antibody (Jackson ImmunoResearch Laboratories; anti-mouse IgG, developed in goat), which was conjugated with FITC in 1:200 dilution with 2% goat serum for 24 h at 4°C. The fluorescence of the stained fibers was monitored using the same confocal setup as used for observing GFP in living fibers.

For dual wavelength imaging of NFATc and the splicing factor SC-35 or the transcription factor MEF2, FDB cultures were first infected with adenovirus-containing NFATc(S $\rightarrow$ A)-GFP for 3 d, and then fixed with parafor-

maldehyde and permeabilized with Triton X-100 as described above. The fibers were then incubated overnight at 4°C with monoclonal antibody against SC-35 (Sigma-Aldrich) diluted 1:300 in 2% goat serum or rabbit polyclonal antibody against MEF2 (reacting with MEF2A and, to a lesser extent, with MEF 2C and 2D, Santa Cruz Biotechnology, Inc.) diluted 1:200 in 2% goat serum. The secondary antibody was goat anti-mouse IgG conjugated with Texas red or donkey anti-rabbit IgG conjugated with Texas red (both from Jackson ImmunoResearch Laboratories). The fluorescence of the stained fibers was viewed with a ZEISS laser scanning confocal microscope. Wavelengths of 488 or 568 nm were used to excite EGFP or Texas red, respectively. Some cultures were infected with NFATc(S→A)-GFP without SC-35 or MEF2 antibody staining, or SC-35 or MEF2 stain without NFATc(S→A)-GFP infection to examine the crosstalk between the two wavelengths used here.

To study the localization of NFATc within the sarcomere, FDB fibers were first infected with NFATc-GFP for 3 d. After fixation and permeabilization, the fibers were incubated with monoclonal antibody against  $\alpha$ -actinin (Sigma-Aldrich) diluted 1:200 in 2% goat serum and then with secondary antibody conjugated with Texas red. Fibers were then imaged on a Biorad Microradiance laser scanning confocal microscope system with wavelengths of 488 or 514 nm for EGFP or Texas red, respectively.

We thank Dr. G.R. Crabtree for providing NFATc and mutant NFATc cDNA and thank Dr. Michael G. Klein and Mr. Patrick Reed for help with dual wavelength imaging of NFATc and  $\alpha$ -actinin, and NFATc SC-35 or MEF2, respectively.

This work was supported by National Institutes of Health grant R01-NS33578 from the National Institute of Neurological Disorders and Stroke.

Submitted: 7 March 2001

Revised: 13 July 2001

Accepted: 13 August 2001

## References

- Abbott, K.L., B.B. Friday, D. Thaloor, T.J. Murphy, and G.K. Pavlath. 1998. Activation and cellular localization of the cyclosporine A-sensitive transcription factor NF-AT in skeletal muscle cells. *Mol. Biol. Cell.* 9:2905–2916.
- Barton-Davis, E.R., W.A. LaFramboise, and M.J. Kushmerick. 1996. Activity-dependent induction of slow myosin gene expression in isolated fast-twitch mouse muscle. *Am. J. Physiol.* 271:C1409–C1414.
- Beals, C.R., N.A. Clipstone, S.N. Ho, and G.R. Crabtree. 1997. Nuclear localization of NF-ATc by a calcineurin-dependent, cyclosporin-sensitive intramolecular interaction. *Genes Dev.* 11:824–834.
- Bekoff, A., and W. Betz. 1977. Properties of isolated adult rat muscle fibres maintained in tissue culture. *J. Physiol.* 271:537–547.
- Bigard, X., H. Sanchez, J. Zoll, P. Mateo, V. Rousseau, V. Veksler, and R. Ventura-Clapier. 2000. Calcineurin Co-regulates contractile and metabolic components of slow muscle phenotype. *J. Biol. Chem.* 275:19653–19660.
- Calvo, S., P. Venepally, J. Cheng, and A. Buonanno. 1999. Fiber-type-specific transcription of the troponin I slow gene is regulated by multiple elements. *Mol. Cell. Biol.* 19:515–525.
- Carroll, S.L., M.G. Klein, and M.F. Schneider. 1997. Decay of calcium transients after electrical stimulation in rat fast- and slow-twitch skeletal muscle fibres. *J. Physiol.* 501:573–588.
- Carroll, S., P. Nicotera, and D. Pette. 1999. Calcium transients in single fibers of low-frequency stimulated fast-twitch muscle of rat. *Am. J. Physiol.* 277: C1122–C1129.
- Chin, E.R., E.N. Olson, J.A. Richardson, Q. Yang, C. Humphries, J.M. Shelton, H. Wu, W. Zhu, R. Bassel-Duby, and R.S. Williams. 1998. A calcineurin-dependent transcriptional pathway controls skeletal muscle fiber type. *Genes Dev.* 12:2499–2509.
- Crabtree, G.R. 1999. Generic signals and specific outcomes: signaling through  $Ca^{2+}$ , calcineurin, and NF-AT. *Cell.* 96:611–614.
- Delling, U., J. Turekova, H.W. Lim, L.J. De Windt, P. Rotwein, and J.D. Molteni. 2000. A calcineurin-NFATc3-dependent pathway regulates skeletal muscle differentiation and slow myosin heavy-chain expression. *Mol. Cell. Biol.* 20:6600–6611.
- Dolmetsch, R.E., R.S. Lewis, C.C. Goodnow, and J.I. Healy. 1997. Differential activation of transcription factors induced by  $Ca^{2+}$  response amplitude and duration. *Nature.* 386:855–888.
- Dunn, S.E., J.L. Burns, and R.N. Michel. 1999. Calcineurin is required for skeletal muscle hypertrophy. *J. Biol. Chem.* 274:21908–21912.
- Dunn, S.E., E.R. Chin, and R.N. Michel. 2000. Matching of calcineurin activity to upstream effectors is critical for skeletal muscle fiber growth. *J. Cell Biol.* 151:663–672.
- Fejes-Toth, G., D. Pearce, and A. Naray-Fejes-Toth. 1998. Subcellular localization of mineralocorticoid receptors in living cells: effects of receptor agonists and antagonists. *Proc. Natl. Acad. Sci. USA.* 95:2973–2978.
- Fowler, A.V., and I. Zabin. 1977. The amino acid sequence of beta-galactosidase of *Escherichia coli*. *Proc. Natl. Acad. Sci. USA.* 74:1507–1510.
- Frey, N., J.A. Richardson, E.N. Olson. 2000. Calcineurin, a novel family of sarcomeric calcineurin-binding proteins. *Proc. Natl. Acad. Sci. USA.* 97:14632–14637.
- Friday, B.B., V. Horsley, and G.K. Pavlath. 2000. Calcineurin activity is required for the initiation of skeletal muscle differentiation. *J. Cell Biol.* 149:657–666.
- Garcia-Cozar, F.J., H. Okamura, J.F. Aramburu, K.T. Shaw, L. Pelletier, R. Shwalter, E. Villafranca, A. Rao. 1998. Two-site interaction of nuclear factor of activated T cells with activated calcineurin. *J. Biol. Chem.* 273:23877–23883.
- Graef, I.A., P.G. Mermelstein, K. Stankunas, J.R. Neilson, K. Deisseroth, R.W. Tsien, and G.R. Crabtree. 1999. L-type calcium channels and GSK-3 regulate the activity of NF-ATc4 in hippocampal neurons. *Nature.* 401:703–708.
- Graham, F.L., and L. Prevec. 1995. Methods for construction of adenovirus vectors. *Mol. Biotechnol.* 3:207–220.
- Hardy, S., M. Kitamura, T. Harris-Stansil, Y. Dai, and M.L. Phipps. 1997. Construction of adenovirus vectors through Cre-lox recombination. *J. Virol.* 71: 1842–1849.
- Hennig, R., and T. Lomo. 1985. Firing patterns of motor units in normal rats. *Nature.* 314:164–166.
- Hoey, T., Y.L. Sun, K. Williamson, and X. Xu. 1995. Isolation of two new members of the NF-AT gene family and functional characterization of the NF-AT proteins. *Immunity.* 2:461–472.
- Hogan, P.G., and A. Rao. 1999. Transcriptional regulation. Modification by nuclear export? *Nature.* 398:200–201.
- Htun, H., J. Barsony, I. Renyi, D.L. Gould, and G.L. Hager. 1996. Visualization of glucocorticoid receptor translocation and intranuclear organization in living cells with a green fluorescent protein chimera. *Proc. Natl. Acad. Sci. USA.* 93:4845–4850.
- Kalderon, D., B.L. Roberts, W.D. Richardson, and A.E. Smith. 1984. A short amino acid sequence able to specify nuclear location. *Cell.* 39:499–509.
- Kanegae, Y., G. Lee, Y. Sato, M. Tanaka, M. Nakai, T. Sakaki, S. Sugano, and I. Saito. 1995. Efficient gene activation in mammalian cells by using recombinant adenovirus expressing site-specific Cre recombinase. *Nucleic Acids Res.* 23:3816–3821.
- Ktistaki, E., N.T. Ktistakis, E. Papadogeorgaki, and I. Talianidis. 1995. Recruitment of hepatocyte nuclear factor 4 into specific intranuclear compartments depends on tyrosine phosphorylation that affects its DNA-binding and transactivation potential. *Proc. Natl. Acad. Sci. USA.* 92:9876–9880.
- Kubis, H.P., E.A. Haller, P. Wetzel, and G. Gros. 1997. Adult fast myosin pattern and  $Ca^{2+}$ -induced slow myosin pattern in primary skeletal muscle culture. *Proc. Natl. Acad. Sci. USA.* 94:4205–4210.
- Lacampagne, A., W.J. Lederer, M.F. Schneider, and M.G. Klein. 1996. Repriming and activation alter the frequency of stereotyped discrete  $Ca^{2+}$  release events in frog skeletal muscle. *J. Physiol.* 497:581–588.
- Lamond, A.I., and W.C. Earnshaw. 1998. Structure and function in the nucleus. *Science.* 280:547–553.
- Lewis, J.D., and D. Tollervy. 2000. Like attracts like: getting RNA processing together in the nucleus. *Science.* 288:1385–1389.
- Liu, Y., and M.F. Schneider. 1998. Fibre type-specific gene expression activated by chronic electrical stimulation of adult mouse skeletal muscle fibres in culture. *J. Physiol.* 512:337–344.
- Liu, Y., S.L. Carroll, M.G. Klein, and M.F. Schneider. 1997. Calcium transients and calcium homeostasis in adult mouse fast-twitch skeletal muscle fibers in culture. *Am. J. Physiol.* 272:C1919–C1927.
- Lomo, T., R.H. Westgaard, and H.A. Dahl. 1974. Contractile properties of muscle: control by pattern of muscle activity in the rat. *Proc. R. Soc. Lond. B. Biol. Sci.* 187:99–103.
- Lopez-Rodriguez, C., J. Aramburu, A.S. Rakeman, and A. Rao. 1999. NFAT5, a constitutively nuclear NFAT protein that does not cooperate with Fos and Jun. *Proc. Natl. Acad. Sci. USA.* 96:7214–7219.
- Luo, C., K.T. Shaw, A. Raghavan, J. Aramburu, F. Garcia-Cozar, B.A. Perrino, P.G. Hogan, and A. Rao. 1996. Interaction of calcineurin with a domain of the transcription factor NFAT1 that controls nuclear import. *Proc. Natl. Acad. Sci. USA.* 93:8907–8912.

- Miska, E.A., C. Karlsson, E. Langley, S.J. Nielsen, J. Pines, T. Kouzarides. 1999. HDAC4 deacetylase associates with and represses the MEF2 transcription factor. *EMBO J.* 18:5099–5107.
- Misteli, T. 2001. Protein dynamics: implications for nuclear architecture and gene expression. *Science.* 291:843–847.
- Miyake, S., M. Makimura, Y. Kanegae, S. Harada, Y. Sato, K. Takamori, C. Tokuda, and I. Saito. 1996. Efficient generation of recombinant adenoviruses using adenovirus DNA-terminal protein complex and a cosmid bearing the full-length virus genome. *Proc. Natl. Acad. Sci. USA* 93:1320–1324.
- Muntener, M., M.W. Berchtold, and C.W. Heizmann. 1985. Parvalbumin in cross-reinnervated and denervated muscles. *Muscle Nerve.* 8:132–137.
- Muntener, M., A.M. Rowlerson, M.W. Berchtold, and C.W. Heizmann. 1987. Changes in the concentration of the calcium-binding parvalbumin in cross-reinnervated rat muscles. Comparison of biochemical with physiological and histochemical parameters. *J. Biol. Chem.* 262:465–469.
- Naya, F.J., B. Mercer, J. Shelton, J.A. Richardson, R.S. Williams, and E.N. Olson. 2000. Stimulation of slow skeletal muscle fiber gene expression by calcineurin in vivo. *J. Biol. Chem.* 275:4545–4548.
- Northrop, J.P., S.N. Ho, L. Chen, D.J. Thomas, L.A. Timmerman, G.P. Nolan, A. Admon, and G.R. Crabtree. 1994. NF-AT components define a family of transcription factors targeted in T-cell activation. *Nature.* 369:497–502.
- Pette, D., and R.S. Staron. 1990. Cellular and molecular diversities of mammalian skeletal muscle fibers. *Rev. Physiol. Biochem. Pharmacol.* 116:1–76.
- Pette, D., and G. Vrbova. 1992. Adaptation of mammalian skeletal muscle fibers to chronic electrical stimulation. *Rev. Physiol. Biochem. Pharmacol.* 120:115–202.
- Pette, D., and R.S. Staron. 1997. Mammalian skeletal muscle fiber type transitions. *Int. Rev. Cytol.* 170:143–223.
- Peuker, H., and D. Pette. 1995. Reverse transcriptase-polymerase chain reaction detects induction of cardiac-like alpha myosin heavy chain mRNA in low frequency stimulated rabbit fast-twitch muscle. *FEBS Lett.* 367:132–136.
- Rao, A., C. Luo, and P.G. Hogan. 1997. Transcription factors of the NFAT family: regulation and function. *Annu. Rev. Immunol.* 15:707–747.
- Salmons, S., and F.A. Sreter. 1976. Significance of impulse activity in the transformation of skeletal muscle type. *Nature.* 263:30–34.
- Schiaffino, S., and C. Reggiani. 1996. Molecular diversity of myofibrillar proteins: gene regulation and functional significance. *Physiol. Rev.* 76:371–423.
- Smith, K.P., P.T. Moen, K.L. Wydner, J.R. Coleman, and J.B. Lawrence. 1999. Processing of endogenous pre-mRNAs in association with SC-35 domains is gene specific. *J. Cell Biol.* 144:617–629.
- Spector, D.L., X.D. Fu, and T. Maniatis. 1991. Associations between distinct pre-mRNA splicing components and the cell nucleus. *EMBO J.* 10:3467–3481.
- Swoap, S.J., R.B. Hunter, E.J. Stevenson, H.M. Felton, N. V. Kansagra, J.M. Lang, K.A. Esser, and S.C. Kandarian. 2000. The calcineurin-NFAT pathway and muscle fiber-type gene expression. *Am. J. Physiol.* 279:C915–C924.
- Timmerman, L.A., N.A. Clipstone, S.N. Ho, J.P. Northrop, and G.R. Crabtree. 1996. Rapid shuttling of NF-AT in discrimination of Ca<sup>2+</sup> signals and immunosuppression. *Nature.* 383:837–840.
- Windisch, A., K. Gundersen, M.J. Szabolcs, H. Gruber, and T. Lomo. 1998. Fast to slow transformation of denervated and electrically stimulated rat muscle. *J. Physiol.* 510:623–632.
- Wu, H., F.J. Naya, T.A. McKinsey, B. Mercer, J.M. Shelton, E.R. Chin, A.R. Simard, R.N. Michel, R. Bassel-Duby, E.N. Olson, R.S. Williams. 2000. MEF2 responds to multiple calcium-regulated signals in the control of skeletal muscle fiber type. *EMBO J.* 19:1963–1973.
- Zhu, J., and F. McKeon. 1999. NF-AT activation requires suppression of Crm1-dependent export by calcineurin. *Nature.* 398:256–260.